HNPS Advances in Nuclear Physics

Vol 30 (2024)

HNPS2023

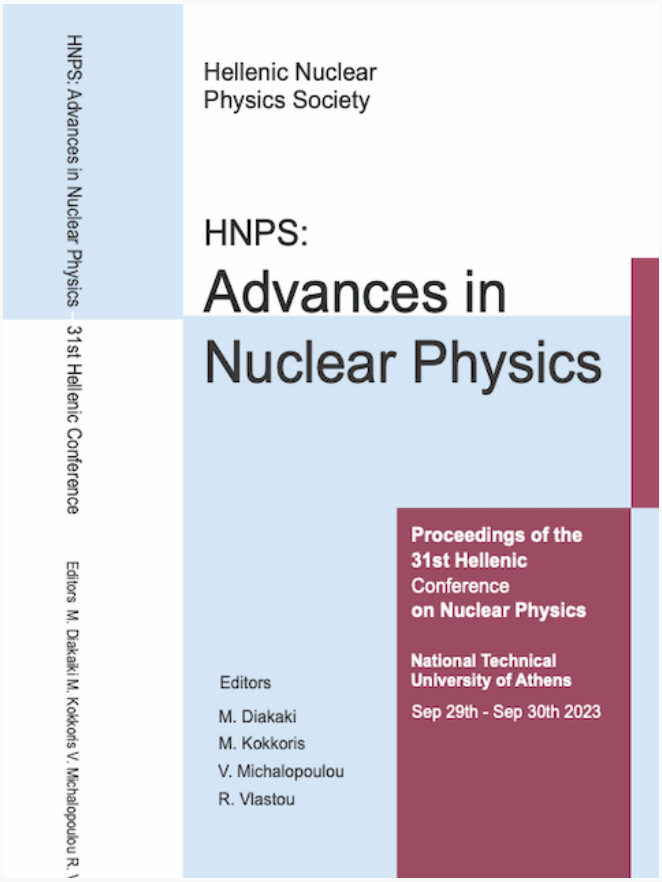

Recent results on elastic scattering and single-neutron stripping reaction in the 18O+48Ti collision at 275 MeV

Onoufrios Sgouros, G. A. Brischetto, F. Cappuzzello, M. Cavallaro, D. Carbone, C. Agodi, D. Calvo, E. R. Chavez Lomeli, I. Ciraldo, M. Cutuli, G. De Gregorio, F. Delaunay, H. Djapo, C. Eke, P. Finocchiaro, M. Fisichella, A. Gargano, M. A. Guazzelli, A. Hacisalihoglu, R. Linares, J. Lubian, N. H. Medina, M. Moralles, J. R. B. Oliveira, A. Pakou, L. Pandola, V. Soukeras, G. Souliotis, A. Spatafora, D. Torresi, A. Yildirim, V. A. B. Zagatto

doi: 10.12681/hnpsanp.6257

Ciraldo, I., Cutuli, M., De Gregorio, G., Delaunay, F., Djapo, H., Eke, C., Finocchiaro, P., Fisichella, M., Gargano, A., Guazzelli, M. A., Hacisalihoglu, A., Linares, R., Lubian, J., Medina, N. H., Moralles, M., Oliveira, J. R. B., Pakou, A., Pandola, L., Soukeras, V., Souliotis, G., Spatafora, A., Torresi, D., Yildirim, A., & Zagatto, V. A. B. (2024). Recent results on elastic scattering and single-neutron stripping reaction in the 18O+48Ti collision at 275 MeV. *HNPS Advances in Nuclear Physics*, *30*, 148–153. https://doi.org/10.12681/hnpsanp.6257

Recent results on elastic scattering and single-neutron stripping reaction in the ^{18}O+^{48}Ti collision at 275 MeV

O. Sgouros[1,2,*], G.A. Brischetto[1,2], F. Cappuzzello[1,2], M. Cavallaro[2], D. Carbone[2], C. Agodi[2], D. Calvo[3], E.R. Chávez Lomelí[4], I. Ciraldo[1,2], M. Cutuli[1,2], G. De Gregorio[5,6], F. Delaunay[1,2,7], H. Djapo[8], C. Eke[9], P. Finocchiaro[2], M. Fisichella[2], A. Gargano[5], M.A. Guazzelli[10], A. Hacisalihoglu[11], R. Linares[12], J. Lubian[12], N.H. Medina[13], M. Moralles[14], J.R.B. Oliveira[13], A. Pakou[15], L. Pandola[2], V. Soukeras[1,2], G. Souliotis[16], A. Spatafora[1,2], D. Torresi[2], A. Yildirim[17], V.A.B. Zagatto[12] for the NUMEN Collaboration

[1] *Dipartimento di Fisica e Astronomia "Ettore Majorana", Università di Catania, Catania, Italy*
[2] *INFN – Laboratori Nazionali del Sud, Catania, Italy*
[3] *INFN – Sezione di Torino, Torino, Italy*
[4] *Instituto de Física, Universidad Nacional Autónoma de México, Mexico City, Mexico*
[5] *INFN – Sezione di Napoli, Napoli, Italy*
[6] *Dipartimento di Matematica e Fisica, Università della Campania "Luigi Vanvitelli", Caserta, Italy*
[7] *LPC Caen UMR6534, Université de Caen Normandie, ENSICAEN, CNRS/IN2P3, Caen, France*
[8] *Institute of Accelerator Technologies, Ankara University, Turkey*
[9] *Department of Mathematics and Science Education, Faculty of Education, Akdeniz University, Antalya, Turkey*
[10] *Centro Universitario FEI, São Bernardo do Campo, Brazil*
[11] *Department of Physics, Recep Tayyip Erdogan University, Rize, Turkey*
[12] *Instituto de Física, Universidade Federal Fluminense, Niterói, Brazil*
[13] *Instituto de Física, Universidade de São Paulo, São Paulo, Brazil*
[14] *Instituto de Pesquisas Energeticas e Nucleares IPEN/CNEN, São Paulo, Brazil*
[15] *Department of Physics, University of Ioannina and Hellenic Institute of Nuclear Physics, Ioannina, Greece*
[16] *Department of Chemistry, University of Athens and Hellenic Institute of Nuclear Physics, Athens, Greece*
[17] *Department of Physics, Akdeniz University, Antalya, Turkey*

Abstract A global study of the ^{18}O+^{48}Ti collision at 275 MeV was carried out within the NUMEN and NURE experimental campaigns by measuring the complete net of nuclear reactions which may be involved in the ^{48}Ti→^{48}Ca double charge exchange transition. The relevant experiment was visualized at the INFN-LNS in Catania, where angular distribution measurements for a plethora of reaction channels were performed by means of the MAGNEX large acceptance magnetic spectrometer. The present work provides an overview of the analyses of the elastic scattering and one-neutron transfer reaction channels.

Keywords Nuclear Reactions, Heavy Ions, Elastic Scattering, Transfer Reactions, Magnetic Spectrometer

INTRODUCTION

Over the past few years, studies for the neutrinoless double beta (0νββ) decay have come to the fore since to date it is considered the best probe of the neutrino nature [1–4]. Numerous large-scale experiments (e.g. [5-7]) participate in a worldwide marathon in prospect of observing such exotic yet elusive process using different nuclei candidates for ββ decay. Such a massive movement is completely justified considering that 0νββ decay is the portal towards the equivalence of neutrino and antineutrino and the neutrino absolute mass scale, provided the experimental half-lifes and the nuclear matrix elements (NMEs) [8,9]. However, our knowledge on the NMEs relies on nuclear structure calculations for determining the nuclear many-body wavefunctions and to date, the values of NMEs are susceptible

* Corresponding author: *onoufrios.sgouros@lns.infn.it*

to large uncertainties leading to vague conclusions on the neutrinos absolute mass scale. On this ground, high quality experimental data to provide the appropriate constraints on the nuclear structure models are highly desirable.

The NUMEN (NUclear Matrix Elements for Neutrinoless double β decay) project [10] consists of a pioneer experimental campaign carried out at Istituto Nazionale di Fisica Nucleare – Laboratori Nazionali del Sud (INFN-LNS) which proposes a new approach on accessing data-driven information on the NMEs of the 0νββ decay. That is to use double charge exchange (DCE) reactions induced by heavy ions for various 0νββ decay candidate targets. In this context, the ^{48}Ti nucleus is of great interest since it is the daughter nucleus of ^{48}Ca in the ββ decay process [11]. The basic point for choosing DCE reactions as probes for studying the 0νββ decay stems from the fact that, despite some differences, the two processes probe the same initial and final-state nuclear wavefunctions [3,10]. Additionally, it has been demonstrated that the NMEs of DCE reactions and those of 0νββ decay can be directly linked, under specific conditions [3,12]. However, in order to obtain meaningful information on the NMEs of the DCE reactions, a detailed description of the complete DCE mechanism is essential.

The DCE mechanism consists of three possible reaction modes: The direct meson-exchange DCE reaction [13,14], two consecutive single charge exchange reactions (DSCE) [15] and the multi-nucleon transfer reactions [16–22]. All these reaction pathways may in principle populate the same final states, but only the first is directly connected to the 0νββ decay. Therefore, it is very important to quantify possible contributions from DSCE and/or multi-nucleon transfer reactions to the measured DCE cross-sections [23], which may be the key for accessing the information on the NMEs of the 0νββ decay [3,4].

Considering all the above, in the present work which is part of the NURE (NUclear REactions for neutrinoless double β decay) project [24], the ^{18}O+^{48}Ti collision was studied at the energy of 275 MeV by measuring in the same experiment elastic and inelastic scattering together with the complete set of the available reaction channels that may contribute to the ^{48}Ti→^{48}Ca transition. The present contribution summarizes the main findings from the analyses of the elastic scattering and ^{48}Ti(^{18}O,^{17}O)^{49}Ti one-neutron transfer reaction [25,26]. The analyses of other reaction channels are ongoing [27].

EXPERIMENTAL DETAILS

The experiment was carried out at the MAGNEX facility [28] of INFN-LNS in Catania. For the needs of the present study, a $^{18}O^{8+}$ ion beam was accelerated at the energy of 275 MeV by the K800 Superconducting Cyclotron and after passing through some series of optical elements it was transported into the scattering chamber and impinged on a TiO_2 target with a thin ^{27}Al backing. Auxiliary measurements using a ^{27}Al target and a WO_3 one with an aluminum backing were also repeated for subtracting the underlying background in the spectra obtained with the TiO_2+^{27}Al target.

The different reaction products were momentum analyzed by the MAGNEX large acceptance magnetic spectrometer [28]. MAGNEX is a high-performance optical spectrometer composed of a large-aperture quadrupole lens followed by a dipole bending magnet, facilitating the detection of charged particles in a wide range of momentum and angles. In the present setup, the optical axis of the spectrometer was set at θ_{opt}= 9º with respect to the beam axis, thus covering an angular range between 3º and 15º in the laboratory reference frame. For the study of the elastic scattering, two additional angular settings were used allowing angular distribution measurements between 3º and 27º in the laboratory reference frame.

The reaction ejectiles were detected by the MAGNEX Focal Plane Detector (FPD) [29], located ~200 cm downstream the exit of the dipole bending magnet. The FPD is composed of two parts namely, a gas detector and a wall of 60 silicon detectors located ~15 mm downstream the gas sector. The use of the gas detector is twofold. It serves as a proportional counter providing the energy loss signal (ΔE_{tot}) of the ions inside the gas, and also as a mean to map the track of the ions inside the gas. The gas detector

is divided in six sections each one having at the top a proportional wire (DC) in which the ΔE signal is measured. Above the DC wires, a set of 6 segmented anode strips is located allowing the measurement of the horizontal position (X_{foc}) and thus, the determination of the horizontal angle (θ_{foc}) at the focal plane. Moreover, the electron drift time measurements inside the gas allow the determination of the vertical position (Y_{foc}) and angle (φ_{foc}). In this way, the reconstruction of the ions trajectories inside the spectrometer can be performed. After crossing the gas sector, the path of the ions is intercepted by the wall of silicon detectors which are used for measuring the residual energy of the ions ($E_{resid.}$). By using the information provided by the silicon detectors in conjunction with the one provided by the gas tracker, the particle identification (PID) is performed following the prescription reported in Ref. [30]. In more details, the different ion species are discriminated among themselves by means of the ΔE-E technique, whereas the different isotopes of the same ion family are separated adopting a technique which is based on the correlation between the kinetic energy of the ions and the measured position along the dispersive direction (X_{foc}). An example of PID spectra is shown in Fig. 1.

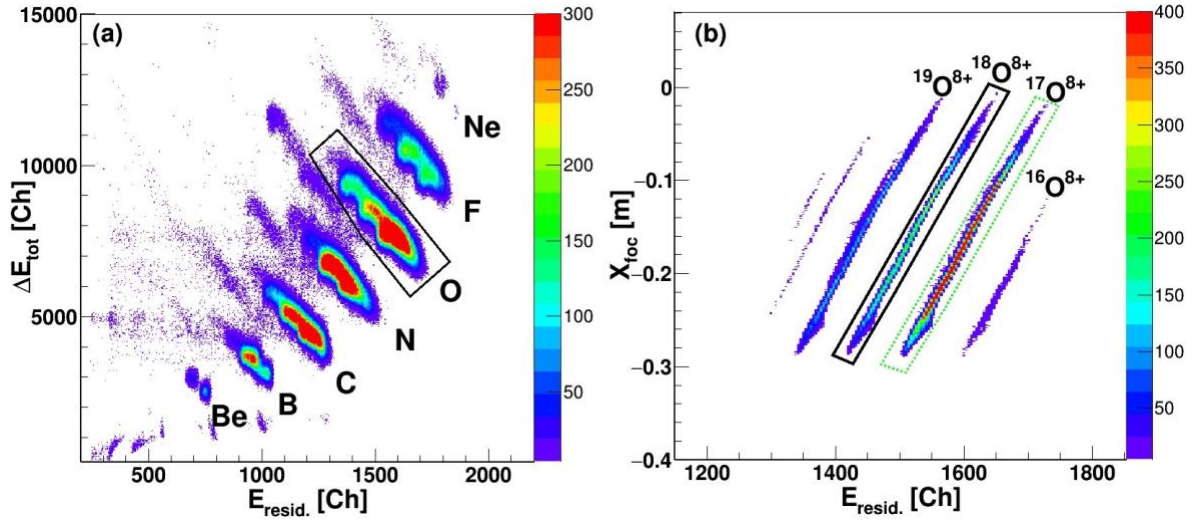

Figure 1. *a) Typical ΔE_{tot} versus residual energy ($E_{resid.}$) correlation plot for a single silicon detector of the FPD. A graphical selection on the oxygen ions is illustrated with the solid black line. b) Horizontal position (X_{foc}) versus $E_{resid.}$ correlation plot after applying the graphical selection on oxygen ions which is depicted in the left panel. The different loci correspond to ions with different ratio m/q². The $^{18}O^{8+}$ and $^{17}O^{8+}$ ions are indicated by the solid black and dashed green contours, respectively.*

DATA REDUCTION AND RESULTS

Having identified the reaction channel of interest, a software trajectory reconstruction was applied to each data set to obtain the initial scattering parameters (θ_i, φ_i, y_i, δ) at the target position from those measured at the reference frame of the FPD (X_{foc}, θ_{foc}, Y_{foc}, φ_{foc}) [31]. A comprehensive description of the trajectory reconstruction for the data set of the one-neutron transfer reaction is given in Ref. [27]. The excitation energy (E_x) of the reactions under study was determined as:

$$E_x = Q_0 - Q, \quad (1)$$

where Q_0 is the ground state (g.s.) to g.s. Q-value calculated from the mass imbalance at the entrance and exit channels and Q is the reaction Q-value calculated adopting the missing mass method [28]. The obtained excitation energy spectra are shown in the panels (a) and (b) of Fig. 2 for the ^{48}Ti(^{18}O,^{18}O)^{48}Ti and the ^{48}Ti(^{18}O,^{17}O)^{49}Ti reactions, respectively. Considering the achieved energy resolution which was about ~500 keV FWHM, from an inspection in Fig. 2a it is seen that the elastic scattering peak is well-separated from other inelastic transitions, while for the case of the one-neutron transfer reaction the g.s. to g.s. transition (labelled as ROI 1) is well-resolved from the rest of the observed structures. In the

latter case, beyond the excitation energy of 1 MeV the level density of ^{49}Ti is appreciably high and therefore, the rest of the observed structures in the spectrum correspond to transitions to various unresolved excited states of ^{17}O and ^{49}Ti nuclei. Having in our possession the energy profile for each reaction, the experimental yields were integrated at each angular range and by taking into account the integrated beam charge during the measurement, the scattering centers of the titanium target, the solid angle and the efficiency of the spectrometer, absolute angle-differential cross-sections were deduced. As representative cases, the angular distribution data corresponding to the elastic scattering and the ROI 3 of the ^{48}Ti(^{18}O,^{17}O)^{49}Ti one-neutron transfer reaction are presented in the panels (a) and (b) of Fig. 3, respectively.

The elastic scattering data were analysed within the Optical Model (OM) and Coupled Channels (CC) frameworks using the FRESCO code [32]. The real and imaginary parts of the optical potential were calculated in a double-folding approach adopting the São Paulo potential (SPP) [33]. In the OM

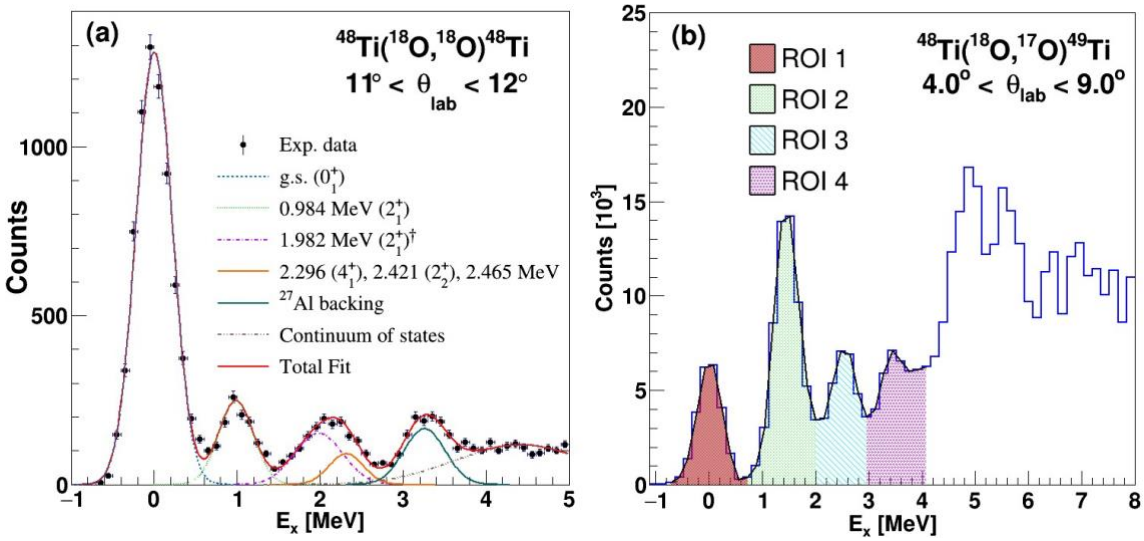

Figure 2. *Reconstructed excitation energy spectrum for the (a) elastic scattering and (b) one-neutron transfer reaction measured at the energy of 275 MeV. In the latter, the spectrum is the one obtained after the background subtraction procedure. Figures are taken from Refs. [25,26].*

calculation, the normalization factors of the real and imaginary parts of the optical potential were fixed to N_R= 1.0 and N_I = 0.78, respectively. Based on systematic studies, it has been shown that the SPP is able to provide a reasonable description of the elastic scattering data for various systems [34-37] in absence of strong coupling effects. However, as it can be seen in Fig. 3a, the OM calculation fails to reproduce the magnitude of the cross-sections at large scattering angles, signalling that coupling effects become important with the increasing angle. To this extent, a CC calculation was also performed taking into account couplings between elastic scattering channel and the low-lying states of the projectile and target nuclei. To model the inelastic excitations the conventional rotational model was used. Moreover, the normalization factor of the imaginary part of the optical potential was reduced to 0.6 to avoid the double counting of the inelastic scattering cross-sections which are explicitly considered in the CC calculation. As it can be seen, the inclusion of couplings significantly improves the agreement between the predicted and the measured cross-sections signalling that the same coupled channels scheme should be adopted in the theoretical description of all other measured reaction channels in the ^{18}O+^{48}Ti collision. An extensive description of the data interpretation is provided in [25].

The ^{48}Ti(^{18}O,^{17}O)^{49}Ti reaction data were analysed using the distorted-waves and coupled-channels Born approximation (DWBA and CCBA) models. The adopted optical potential at the entrance channel

was the one deduced from the analysis of the elastic scattering data, while the exit channel and core-core potentials were calculated adopting the SPP with the standard normalization factors. The spectroscopic amplitudes for the $<^{17}O|^{18}O>$ and $<^{49}Ti|^{48}Ti>$ overlaps were calculated with large-scale shell-model calculations using the KSHELL code [38]. In more details, the calculation of the spectroscopic amplitudes for the projectile overlaps was performed adopting the p-sd-mod interaction [39], while for the target overlaps adopting the SDPF-MU interaction [40]. The results of the theoretical calculations are compared to the experimental data in Fig. 3b. The CCBA calculation yielded almost identical results to those obtained with the DWBA one suggesting that the involved states are characterized by a substantial single-particle strength. However, both calculations overestimate the magnitude of the experimental data by a factor of ~2. This discrepancy is attributed to a large cross-section predicted for the $(5/2^-)_3$ state of the ^{49}Ti nucleus at 2.261 MeV, associated to the large value of the predicted spectroscopic amplitude compared to the experimental values [41]. This hypothesis is well borne-out by the results of a preliminary shell-model calculation adopting the KB3 interaction [42], where a smaller value of the spectroscopic amplitude for this state is predicted. Using the results of this new calculation, it can be seen that the agreement between data and theory is significantly improved. An extensive description of the data interpretation is provided in [26].

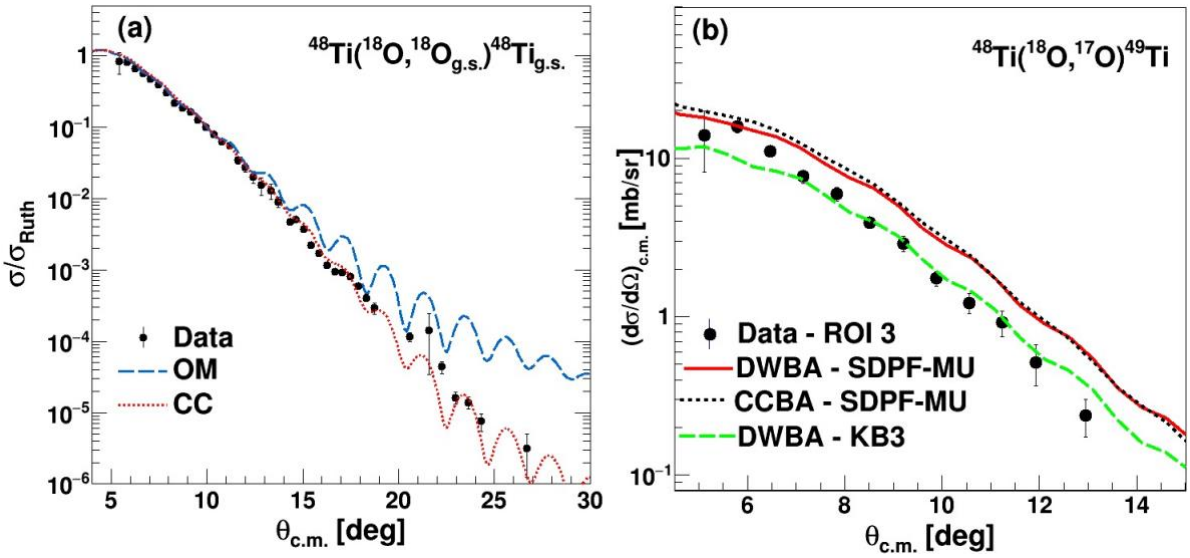

Figure 3. *(a) Elastic scattering angular distribution data for the $^{18}O+^{48}Ti$ collision at 275 MeV. The experimental data, indicated by the black points, are compared to the results of an optical model (OM) and a coupled channels (CC) calculation which is illustrated with the dashed blue and dotted red line, respectively. (b) Angular distribution data for the $^{48}Ti(^{18}O,^{17}O)^{49}Ti$ reaction at 275 MeV. The experimental data, indicated by the black points, are compared to the results of DWBA and CCBA calculations which are illustrated with the colored curves. Figures are taken from Refs. [25,26].*

CONCLUSIONS

A global study of the $^{18}O+^{48}Ti$ collision at 275 MeV was pursued as part of the NUMEN and NURE experimental campaigns aiming at measuring the complete net of the available direct reactions. Angular distribution measurements for a plethora of reaction channels were performed by means of the MAGNEX large acceptance magnetic spectrometer at INFN-LNS. The present work highlights the recent results obtained from the analyses of the elastic scattering and one-neutron transfer reaction. The analysis of the elastic scattering data showed that couplings to the low-lying states of the projectile and target nuclei have important influence on the predicted elastic scattering cross-sections and therefore, should be explicitly taken into account in the theoretical interpretation of other direct reactions in the

^{18}O+^{48}Ti collision. On this ground, the same initial state interaction (optical potential+coupling scheme) was invoked for the theoretical interpretation of the ^{48}Ti(^{18}O,^{17}O)^{49}Ti one-neutron transfer reaction, where a substantial sensitivity of the differential cross-sections on different nuclear structure models was inferred. This result provides an important input to the analysis of the DCE reaction, underlining that special attention should be given to the choice of the nuclear structure model for an accurate description of the wavefunctions of the involved nuclei, with major consequences in the determination of the NMEs for the ββ decay process.

Acknowledgments

This project has received financial support from the European Research Council (ERC) under the European Union's Horizon 2020 Research and Innovation Programme (NURE - Grant agreement No. 714625).

References

[1] J. Barea et al., Phys. Rev Lett. 109, 042501 (2012), doi: 10.1103/PhysRevLett.109.042501
[2] J.D. Vergados et al., Int. J. Mod. Phys. E 25, 1630007 (2016), doi: 10.1142/S0218301316300071
[3] H. Lenske et al., Prog. Part. Nucl. Phys. 109, 103716 (2019), doi: 10.1016/j.ppnp.2019.103716
[4] F. Cappuzzello et al., Prog. Part. Nucl. Phys. 128, 103999 (2023), doi: 10.1016/j.ppnp.2022.103999
[5] J.B. Albert et al., Nature 510, 229 (2014), doi: 10.1038/nature13432
[6] A. Gando et al., Phys. Rev. Lett. 117, 082503 (2016), doi: 10.1103/PhysRevLett.117.082503
[7] M. Agostini et al., Phys. Rev. Lett. 125, 252502 (2020), doi: 10.1103/PhysRevLett.125.252502
[8] J. Engel et al., Rep. Prog. Phys. 80, 046301 (2017), doi: 10.1088/1361-6633/aa5bc5
[9] H. Ejiri et al., Phys. Rep. 797, 1 (2019), doi: 10.1016/j.physrep.2018.12.001
[10] F. Cappuzzello et al., Eur. Phys. J. A 54, 72 (2018), doi: 10.1140/epja/i2018-12509-3
[11] A. Belley et al., Phys. Rev. Lett. 126, 042502 (2021), doi: 10.1103/PhysRevLett.126.042502
[12] E. Santopinto et al., Phys. Rev. C 98, 061601(R) (2018), doi: 10.1103/PhysRevC.98.061601
[13] F. Cappuzzello et al., Eur. Phys. J. A 51, 145 (2015), doi: 10.1140/epja/i2015-15145-5
[14] V. Soukeras et al., Results in Physics 28, 104691 (2021), doi: 10.1016/j.rinp.2021.104691
[15] M. Cavallaro et al., Front. Astron. Space Sci. 8, 659815 (2021), doi: 10.3389/fspas.2021.659815
[16] D. Carbone et al., Phys. Rev. C 102, 044606 (2020), doi: 10.1103/PhysRevC.102.044606
[17] J.L. Ferreira et al., Phys. Rev. C 103, 054604 (2021), doi: 10.1103/PhysRevC.103.054604
[18] O. Sgouros et al., Phys. Rev. C 104, 034617 (2021), doi: 10.1103/PhysRevC.104.034617
[19] S. Calabrese et al., Phys. Rev. C 104, 064609 (2021), doi: 10.1103/PhysRevC.104.064609
[20] I. Ciraldo et al., Phys. Rev. C 105, 044607 (2022), doi: 10.1103/PhysRevC.105.044607
[21] S. Burrello et al., Phys. Rev. C 105, 024616 (2022), doi: 10.1103/PhysRevC.105.024616
[22] A. Spatafora et al., Phys. Rev. C 107, 024605 (2023), doi: 10.1103/PhysRevC.107.024605
[23] J.L. Ferreira et al., Phys. Rev. C 105, 014630 (2022), doi: 10.1103/PhysRevC.105.014630
[24] M. Cavallaro et al., PoS BORMIO 2017, 015 (2017), doi: 10.22323/1.302.0015
[25] G.A. Brischetto et al., Phys. Rev. C 109, 014604 (2024), doi: 10.1103/PhysRevC.109.014604
[26] O. Sgouros et al., Phys. Rev. C 108, 044611 (2023), doi: 10.1103/PhysRevC.108.044611
[27] O. Sgouros, Il Nuovo Cimento 45 C, 70 (2022), doi: 10.1393/ncc/i2022-22070-3
[28] F. Cappuzzello et al., Eur. Phys. J. A 52, 167 (2016), doi: 10.1140/epja/i2016-16167-1
[29] D. Torresi et al., Nucl. Instrum. Meth. A 989, 164918 (2021), doi: 10.1016/j.nima.2020.164918
[30] F. Cappuzzello et al., Nucl. Instrum. Meth. A 621, 419 (2010), doi: 10.1016/j.nima.2010.05.027
[31] F. Cappuzzello et al., Nucl. Instrum. Methods A 638, 74 (2011), doi: 10.1016/j.nima.2011.02.045
[32] I.J. Thompson, Comput. Phys. Rep. 7, 167 (1988), doi: 10.1016/0167-7977(88)90005-6
[33] M.A. Candido Ribeiro et al., Phys. Rev. Lett 78, 3270 (1997), doi: 10.1103/PhysRevLett.78.3270
[34] D. Pereira et al., Nucl. Phys. A 826, 211 (2009), doi: 10.1016/j.nuclphysa.2009.06.015
[35] D. Pereira et al., Phys. Lett. B 710, 426 (2012), doi: 10.1016/j.physletb.2012.03.032
[36] L.M. Fonseca et al., Phys. Rev. C 100, 014604 (2019), doi: 10.1103/PhysRevC.100.014604
[37] A. Spatafora et al., Phys. Rev. C 100, 034620 (2019), doi: 10.1103/PhysRevC.100.034620
[38] N. Shimizu et al., Comput. Phys. Commun. 244, 372 (2019), doi: 10.1016/j.cpc.2019.06.011
[39] Y. Otsuno et al., Phys. Rev. C 83, 021301(R) (2011), doi: 10.1103/PhysRevC.83.021301
[40] Y. Otsuno et al., Phys. Rev. C 86, 051301(R) (2012), doi: 10.1103/PhysRevC.86.051301
[41] A.E. Ball et al., Nucl. Phys. A 183, 472 (1972), doi: 10.1016/0375-9474(72)90351-X
[42] A. Poves and A. Zuker, Phys. Rep. 70, 235 (1981), doi: 10.1016/0370-1573(81)90153-8